ELSEVIER

Journal of Photochemistry and Photobiology A: Chemistry 146 (2001) 75–81

Journal of Photochemistry and Photobiology A:Chemistry

www.elsevier.com/locate/jphotochem

Photophysical properties of two new psoralen analogs

Antonio Eduardo da Hora Machado [a,*], Jacques Antonio de Miranda [a], Ana Maria Ferreira de Oliveira-Campos [b], Divinomar Severino [c], David Ernest Nicodem [c]

[a] *Laboratório de Fotoquímica/GFQL, Instituto de Química, Universidade Federal de Uberlândia, P.O. Box 593, Uberlândia, 38400-089 Minas Gerais, Brazil*

[b] *Centro de Química, Universidade do Minho, IQBF, Campus Gualtar, P-4700 Braga, Portugal*

[c] *Laboratório de Espectroscopia Resolvida no Tempo, Instituto de Química, Universidade Federal do Rio de Janeiro, CEP 21949-900 Rio de Janeiro, RJ, Brazil*

Received 4 June 2001; accepted 22 August 2001

Abstract

The photophysics of two new psoralen analogs has been examined using absorption and emission spectroscopy. Both compounds efficiently absorb radiation in the UVA region ($320 < \lambda < 400$ nm) which are weakly fluorescent and sensitize the generation of singlet oxygen with a quantum efficiency near unity. © 2001 Elsevier Science B.V. All rights reserved.

Keywords: Psoralens; Quantum efficiency; Singlet oxygen

1. Introduction

Psoralens are plant natural products. They are coumarin derivatives. Their basic characteristic is a furanic ring fused to the coumarin basic structure [1] (Scheme 1). They are often photosensitizing drugs, and widely used for the treatment of various skin diseases characterized by hyperproliferative conditions [1–4], some infections connected to AIDS [5] and blood decontamination [6]. Therapy involves the combination of drug administration and UVA light ($320 < \lambda < 400$ nm). However, the treatment with these drugs may be accompanied by some serious side effects, such as skin phototoxicity and mutagenicity [3,7,8]. The photobiological activity of psoralens is basically related to their capacity to damage DNA. In the dark, these compounds can intercalate into DNA base pairs, forming weak molecular complexes, which generally do not induce significant biological effects [2]. However, upon exposing such complexes to UVA light, they photoreact with the pyrimidine bases of DNA, forming covalent mono- and bifunctional C_4 cycloadducts [2], by a type III mechanism. Besides type III, psoralens can photosensitize type I and II reactions [1a]. Type I and II reactions are, electron-transfer and energy-transfer oxygen-mediated reactions respectively. In the first reaction, radicals such as superoxide are generated as reactive intermediates, and in type II, singlet oxygen is produced [9]. Type III reaction consists of photoreactions between the psoralen and substrate, and is favored by polar solvents. In general, the C_3C_4 and $C_4'C_5'$ double bonds are photoreactives, but in solution only the C_3C_4 is involved, showing that this bond is particularly reactive in the triplet state [1]. The three mechanisms are involved in the induction of damage to membrane constituents [1a, 10].

The substitution of hydrogens in the positions 3, 4, 4′ and 5′ by groups greater in volume or having electron-withdrawing properties can reduce the photoreactivity of the active double bonds, and impose limits to the intercalation capacity of these compounds [1a]. Bordin et al. [10] have studied the biological and photochemical activities of 4-hydroxymethyl-4′,5′-tetrahydro-benzopsoralen, a compound quite similar to the analogs studied in this paper. This compound induced strong antiproliferative effects in the dark and under illumination with UVA light. In the dark, it inhibited the synthesis of DNA and RNA in cells, and under illumination, demonstrated good singlet oxygen sensitizing capability. Also under UVA, the synthesis of DNA was inhibited.

In this work, the photophysical properties of two psoralen analogs, 3-ethoxycarbonyl-2H-benzofuro[2,3-e]-1-benzopyran-2-one (pso A), and 3-ethoxycarbonyl-2H-benzofuro-[3,2-d]-1-benzopyran-2-one (pso B) are presented (Fig. 1). Particularly, both compounds sensitize the generation of singlet oxygen with a quantum yield near unity.

* Corresponding author.
E-mail address: aeduardo@ufu.br (A.E. da Hora Machado).

1010-6030/01/$ – see front matter
PII: S1010-6030(01)00552-4

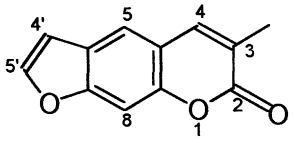

Scheme 1. A typical psoralen.

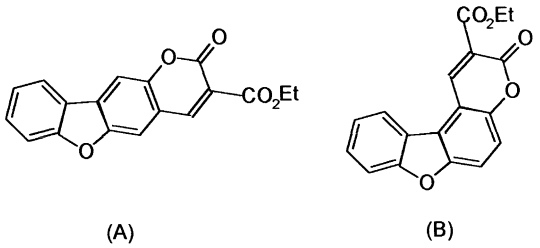

Fig. 1. Representation of the two psoralens under study: (A) 3-ethoxycarbonyl-2H-benzofuro[2,3-e]-1-benzopyran-2-one (pso A); (B) 3-ethoxycarbonyl-2H-benzofuro[3,2-d]-1-benzopyran-2-one (pso B).

2. Experimental

2.1. Materials

All the solvents were of spectroscopic grade. Chloroform was treated with activated silica for 12 h before its use in the measurements of quantum yield of $^1O_2$ generation. The synthesis and characterization of the two psoralen analogs was carried out by Oliveira-Campos and co-workers, and will be published in a separate paper.

2.2. Measurements and methods

Absorption and emission spectra were recorded, on a HACH DR-4000U spectrophotometer and a HITACHI F-4500 spectrofluorometer, respectively, equipped with low-temperature accessories. The fluorescence spectra were obtained, using a right angle configuration in the sample compartment, by exciting the sample at the wavelength of maximum absorption. The fluorescence quantum yield was determined from the corrected fluorescence spectra with 9,10-diphenylantracene in cyclohexane ($\Phi_{fl} = 0.90$ at 20°C) as standard, using the equation below [11]

$$\phi_a = \frac{A_s F_a n_a^2}{A_a F_s n_s^2}\phi_s$$

where ϕ_a and ϕ_s are the quantum yields of the sample and of the standard, respectively, A the absorbance at the excitation wavelength, F the integrated emission area and n the refractive index of the solvent. The absorbance of the solutions, including the standard at the wavelength of excitation, was maintained below 0.100.

The fluorescence lifetimes were obtained by the use of a time-correlating single photon counting technique through a CD-900 Edinburgh Analytical Instrument, using a front face configuration in the sample compartment. The excitation source was a hydrogen-filled nanosecond flash lamp at 30 kHz pulse frequency. The χ^2-values were $0.950 < \chi^2 < 1.010$.

The quantum efficiencies of singlet oxygen generation and triplet lifetimes were quantified for both psoralens in chloroform, for solutions with absorbance of 0.300 at 355 nm. A front-surface configuration was used for both sample and standard for the measurements of quantum efficiencies of singlet oxygen generation. For the triplet lifetime measurements, a right angle configuration was used. An LP 900 Edinburgh Analytical Instruments time-resolved system, using 5 ns laser pulses at 355 nm furnished by a Nd-YAG CONTINUUM SURELITE II (Q-switched delay 200 μs) was used. The laser power varied from 0 to 8 mJ. A NORTH COAST EO-817 detector was used for the detection of singlet oxygen phosphorescence at 1270 nm. For the measurement of triplet lifetimes, the laser power was 30–40 mJ (confirmar), and an R955 photomultiplier was used to detect the transient signals. The transient absorption was investigated between 380 and 600 nm for solutions previously deaerated, and the decays were monitored at the transient absorption maximum for each sample. The quantum efficiency of singlet oxygen generation was determined using phenalenone in chloroform ($\phi_{\Delta,s} = 0.97 \pm 0.02$ at 20°C) as standard, due to its photophysical parameters, including $\Phi_\Delta \approx 1$, for different solvents, following is the equation [12],

$$\phi_{\Delta,a} = \frac{I_a}{I_s}\phi_{\Delta,s}$$

where I_a is the emission intensity of the sample, I_s the emission intensity of the standard and $\phi_{\Delta,a}$ the quantum efficiency of singlet oxygen generation by the sample. The samples and standard were excited at different laser pulse energies, and the initial intensity of emission at 1270 nm was measured. The ratio I_a/I_s is calculated from the slopes of the plot of signal intensity vs. laser pulse energy.

The energy and multiplicity of the excited states were calculated for both compounds using configuration interaction (CI). The structures were previously optimized using the Polar-Ribiere algorithm. The RMS gradient was limited to 0.1 kcal/(Å mol) as convergence limit. All calculations were based on the PM3 semiempirical method (Hyperchem Pro 5.11). These calculations were performed using a PC based on a 450 MHz Intel Pentium III processor, with 196 MB of 100 MHz SDRAM.

3. Results and discussion

3.1. Absorption and emission spectra

The absorption spectra of both compounds are quite similar, with two intense bands. Psoralen A (pso A) shows maxima at 208 and 347 nm, while psoralen B (pso B) exhibits bands at 202 and 349 nm (Fig. 2). All are attributed to

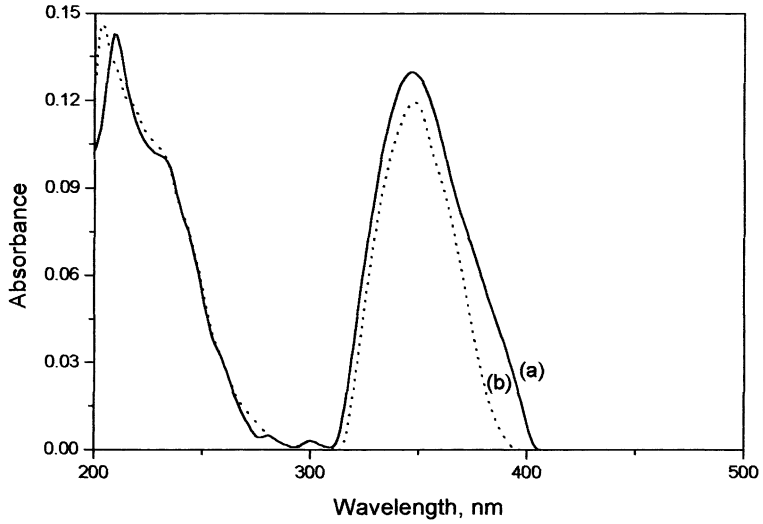

Fig. 2. Absorption spectra: (a) pso A (2.71×10^{-6} mol/dm^3); (b) pso B (5.18×10^{-6} mol/dm^3). Solvent: chloroform.

$\pi\pi^*$ transitions of electrons in the psoralen ring. A shoulder at approximately 235 nm is also seen for both the compounds. A very small peak around 300 nm, attributed to an $n\pi^*$ transition from the non-bonding orbital on the C_2 carbonyl group to the π^* orbital can be also seen. The peaks centered around 348 nm present high molar absorptivity (10^4 dm^3 mol^{-1} cm^{-1}) for both compounds. The log ε for that transition is 4.68 and 4.36 for pso A and pso B, respectively, in chloroform. This high ε is in agreement with an expected $\pi\pi^*$ $S_0 \rightarrow S_1$ transition, characteristic of this class of compounds [1a].

3.2. Fluorescence and phosphorescence

Despite the very intense absorption at $S_0 \rightarrow S_1$ electronic transition, the fluorescence spectra are of low intensity, with small Φ_F: 0.020 for pso A and 0.010 for pso B. At 77 K, these values increase at least five times (0.100 for pso A and 0.064 for pso B). Assuming that the only photophysical processes occurring from S_1 for both compounds are fluorescence and intersystem crossing, and observing that the quantum yield of fluorescence increases at low temperature, a slight thermal activation energy to intersystem crossing could be involved. Using the data at room temperature and 77 K, activation energies of ISC of 6.14 and 6.90 J/mol can be calculated for pso A and pso B, respectively. This rough estimation suggests that the triplet state populated by the S_1 state is slightly higher in energy. The pre-exponential values which would be the rate in the absence of an activation energy are $2–4 \times 10^9$ and are reasonable for a $\pi\pi^*$ singlet to $n\pi^*$ triplet transition. The data from CI quantum mechanical calculations indicates that the intersystem crossing must occur from S_1 to a T_2 excited state for both the compounds, isolated or solvated, being $E(T_2) < E(S_1)$ (Table 1). In the calculations involving solvation, chloroform was considered as solvent.

As can be seen from Table 1, the theoretical values, calculated for $E(S_1)$ and $E(T_1)$ considering the solvation of the molecules, are higher than the experimental ones. However, these differences show a certain regularity. For pso A, it is around 30% for both states. For pso B, the differences are lower, between 13.5% for $E(T_1)$ and 19.4% for $E(S_1)$. Considering a difference of 30% between the theoretical prevision and the experimental value

Table 1
Microstates of the pso A and pso B, calculated using PM3 semi-empirical calculation, and estimated from low temperature measurements

State	Relative energy (kJ/mol)					
	Pso A			Pso B		
	PM3 (isolated)[a]	PM3 (solvated)[b]	Experimental	PM3 (isolated)[a]	PM3 (solvated)[b]	Experimental
S_0	0.00	0.00	0.00	0.00	0.00	0.00
T_1	284.83	302.92	231.24	269.57	265.39	233.74
T_2	320.94	332.60	255.85[c]	308.28	304.39	254.93[c]
S_1	348.49	370.81	292.01	346.73	340.34	284.91

[a] Isolated: 400 configurations.
[b] Solvated: 4900 configurations.
[c] Theoretical prevision of $E(T_2)$.

for pso A, we can speculate on an experimental value for $E(T_2)$ as being 255.85 kJ/mol. Thus, the difference $E(S_1)-E(T_2)$ must be around 36.16 kJ/mol. This difference is very near to the theoretical values, 38.21 kJ/mol. For pso B, considering a difference of 19.4% between the theoretical prevision and the experimental values, we can approach an experimental value of 254.93 kJ/mol for $E(T_2)$. Thus, the difference $E(S_1)-E(T_2)$ must be around 30.06 kJ/mol in this case. The difference between the theoretical data is 35.95 kJ/mol. For both the compounds, these small differences justify an efficient population of the T_2 state.

The simulation of the solvated molecules was done using 4900 configurations to compensate the inclusion of the solvent in the calculation. Eighteen molecules of chloroform were arranged around each molecule of psoralen. The CI calculations for the isolated molecules were done using 400 configurations. Even considering an intermediate number of configurations in the expression of the solvated molecule, the results do not differed substantially from that obtained with 4900 configurations. The theoretical behavior is in agreement with the experimental one, principally if we consider the facility presented by these species to populate the T_1 state, as can be seen by the ratio k_{ST}/k_F.

Assuming that for the deactivation of the S_1 excited state of pso A and pso B, we have

$$\Phi_F = k_F(k_F + k_{ST})^{-1} = k_F\tau_{exp}$$

As Φ_F is small, then $k_{ST} > k_F$ and the above expression can be resumed to

$$\Phi_F = \frac{k_F}{k_{ST}} = k_F\tau_{exp}$$

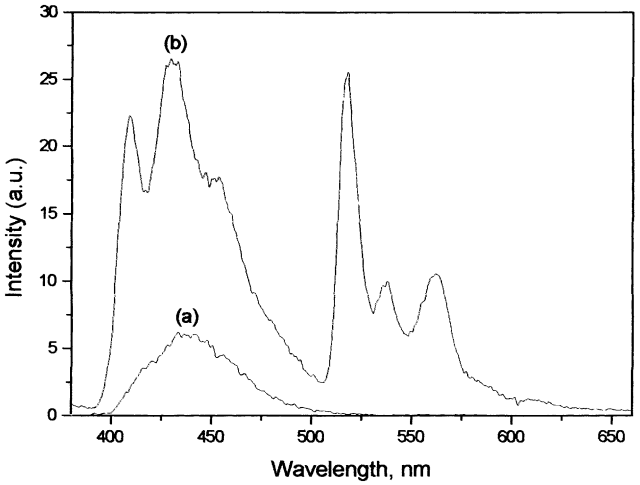

Fig. 3. Emission spectra: (a) fluorescence spectrum for pso A at 300 K; (b) total emission spectrum for pso A at 77 K. Solvent: methyl-cyclohexane; excitation wavelength: 354 nm; concentration: 2.71×10^{-6} mol/dm^3.

The experimental lifetimes, τ_{exp}, are 0.385 ± 0.006 and 0.766 ± 0.007 ns for pso A and pso B, respectively, in chloroform. The calculated fluorescence lifetimes are 19.25 and 76.60 ns, respectively.

Based on the above expression, we can estimate k_F and k_{ST} for both the compounds: pso A, $k_F = 5.2 \times 10^7\ s^{-1}$ and $k_{ST} = 2.6 \times 10^9\ s^{-1}$; pso B, $k_F = 1.3 \times 10^7\ s^{-1}$ and $k_{ST} = 1.3 \times 10^9\ s^{-1}$. Then $k_{ST} \approx 50k_F$ for pso A, and $k_{ST} \approx 100k_F$ for pso B, which agrees with the small values found for Φ_F. As is known, the presence of a carbonyl group in the conjugated aromatic structures tends to favor k_{ST} [13].

As can be seen from Figs. 3 and 4, at 77 K, the phosphorescence spectra are well resolved for both species: the spectra are similar, showing three peaks, the first attributed

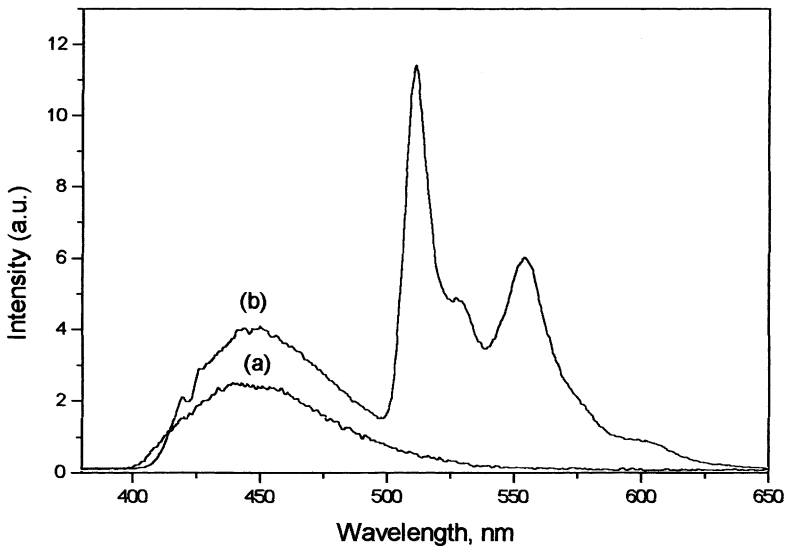

Fig. 4. Emission spectra: (a) fluorescence spectrum for pso B at 300 K; (b) total emission spectrum for pso B at 77 K. Solvent: methyl-cyclohexane; excitation wavelength: 348 nm; concentration: 5.18×10^{-6} mol/dm^3.

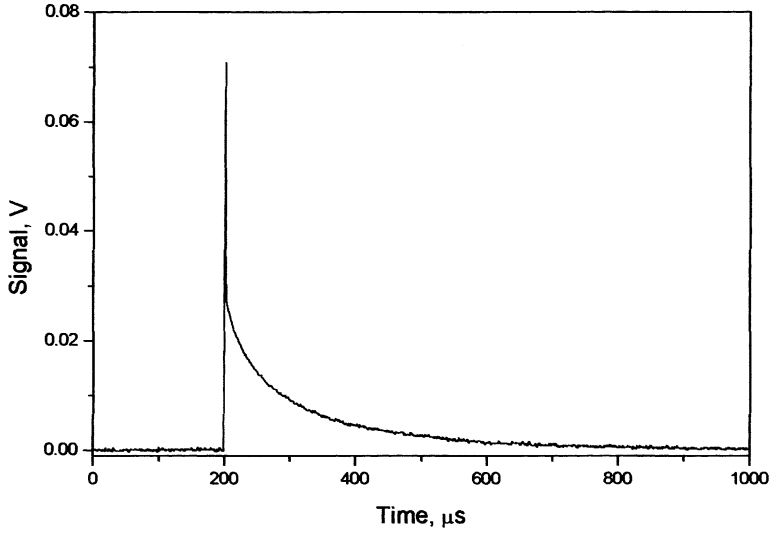

Fig. 5. Typical singlet oxygen emission decay at 1270 nm generated by pso B. Solvent: chloroform.

to $T_{1,0} \rightarrow S_{0,0}$. For pso A, $E_T = 231.24$ kJ/mol and pso B, 233.75 kJ/mol. The experimental S_1 energies are 292.01 and 284.91 kJ/mol, for pso A and pso B, respectively (Table 1).

3.3. Singlet oxygen generation

The quantum yield of $^1O_2$ generation by sensitization in non-aqueous solvents can be conveniently measured using the near-IR phosphorescence of singlet oxygen around 1270 nm, of a sample relative to a standard [9,12,14]. Since the radiation rate constant of singlet oxygen depends on the solvent [5], it is necessary to compare the emissions of the investigated sensitizer and the reference sensitizer dissolved in a same solvent. At low laser pulse energies, the intensity at $t = 0$ s in a time-resolved emission decay is proportional to the amount of singlet oxygen generated and to the laser pulse energy.

Fig. 5 shows a typical profile of that decay. The initial amplitude of this signal is proportional to the yield of singlet oxygen. Under our experimental conditions, the decay of this signal, which reflects the lifetime of singlet oxygen is consistent with the value reported in the literature for chloroform [9]. The lifetime calculated was of 1.94×10^{-4} s ($\chi^2 \approx 0.97$) in chloroform, for both the compounds.

Initial emission intensities of the standard (phenalenone) and the samples were measured at different laser pulse energies. These values were plotted against the laser pulse energy. The ratio of the slopes is equal to the ratio of the quantum yields at low laser pulse energies where the signal is directly proportional to the pulse energy. This methodology gives a more accurate evaluation I_a/I_s than would be possible using measurement at a single pulse energy, and guarantees that neither signal is saturating

$$\frac{I_a}{I_s} \approx \frac{(\Delta S/\Delta P)_a}{(\Delta S/\Delta P)_s} = \frac{(\Delta S)_a}{(\Delta S)_s}$$

$(\Delta P)_a = (\Delta P)_s$, considering that the experiments are done under the same conditions.

Fig. 6 shows the energy dependence plot, obtained for phenalenone, pso A and pso B. The slopes, estimated by linear fit ($R > 0.99$), for phenalenone, pso A and pso B, in the range between 0.0 and 3.0 mJ, were, respectively, 1.3692, 1.3704 and 1.3319 V J^{-1}. From these values, and the previous value of $\phi_{\Delta,s}$ (0.97 at 20°C) for phenalenone [12], the quantum yields of singlet oxygen generation from pso A and

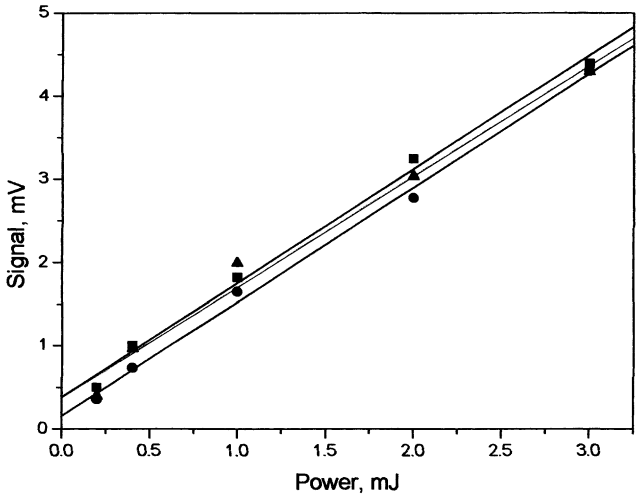

Fig. 6. Power dependence plot for: (■) phenalenone; (▲) pso A; (●) pso B ($R > 0.99$); emission at 1270 nm; excitation at 355 nm; solvent: chloroform.

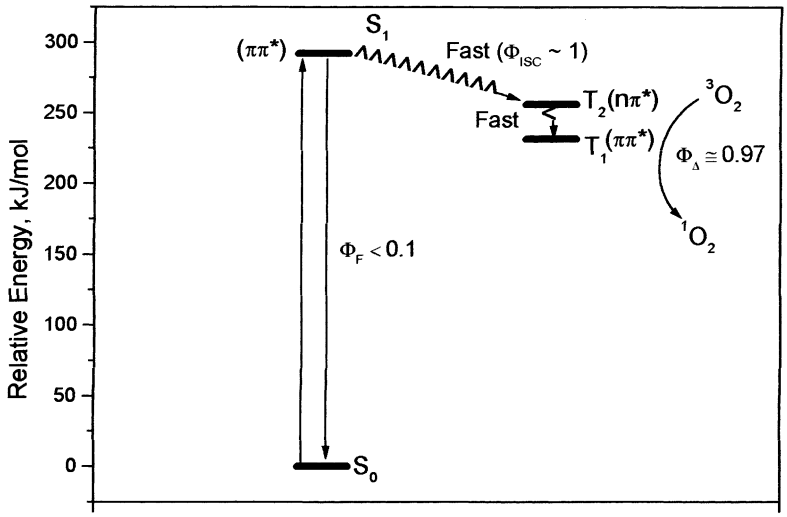

Scheme 2. Representation of the first microstates for pso A.

pso B were 0.97 ± 0.06 and 0.94 ± 0.06, respectively. These are high values, comparable to the best singlet oxygen sensitizers and much higher than that found for other psoralens [4,9a].

Considering the absorption spectra in chloroform, these compounds should efficiently sensitize the singlet oxygen formation under natural sunlight. The values of Φ_Δ estimated for both the compounds indicate that the T_1 state responsible for the singlet oxygen generation is a ketonic $\pi\pi^*$ excited state, which generally displays a high efficiency for singlet oxygen formation [15–17]. Also, the elevated triplet lifetimes, estimated by flash photolysis measurements, 37 ± 3 and $22 \pm 1\,\mu s$, respectively for pso A and pso B are sufficiently high to justify the T_1 state as $\pi\pi^*$. These transients absorb with maxima around 470 nm for pso A, and 480 nm for pso B. As the theoretical calculation results show that this state is populated by internal conversion from a T_2 excited state, which is populated by intersystem crossing from S_1 state. It is possible that the T_2 state is an $n\pi^*$ state, as occurs also with phenalenone [18]. It is pertinent to consider that ϕ_{ISC} is near unity, considering the values observed for the ratio k_{ST}/k_F. Similarly, in phenalenone ϕ_{ISC} between S_1 and $T_2(n\pi^*)$ is around the unity and occurs in a timescale around 10^{-9} s [17]. Schematically, for both the compounds, an energy diagram could be represented as shown in Scheme 2. Singlet oxygen formation cannot occur from the singlet state as the singlet excited states of these compounds are too short to allow quenching by intermolecular oxygen diffusion. The singlet–triplet energy gap is also too small to allow singlet oxygen formation through oxygen-induced intersystem crossing. The near unity quantum yield of singlet oxygen formation, therefore, indicates that the triplet yield is also near one and that the principal photophysical process for decay of the singlet excited state is intersystem crossing.

Although the prediction of the state energies are considerably higher than the experimental ones, these predictions can be considered sufficiently safe, considering that these results are referred to semi-empirical calculations.

Acknowledgements

CNPq, CAPES, FAPEMIG and FINEP are greatly acknowledged.

References

[1] F. Dall'Acqua, D. Vedaldi, S. Caffieri, in: H. Hönigsmann, G. Jori, A.R. Young (Eds.), The Fundamental Bases of Phototherapy, OEMF, Milano, 1996, pp. 1–16.
[2] F. Bordin, Int. J. Photoenergy 1 (1999) 1.
[3] S. Mobilio, L. Tondelli, M. Capobianco, O. Gia, Photochem. Photobiol. 61 (1995) 113.
[4] S.C. Shim, in: W.M. Horspool, P.-S. Song (Eds.), CRC Handbook of Organic Photochemistry and Photobiology, CRC Press, Boca Raton, FL, 1995 (Chapter 8).
[5] J. Gorin, M. Lessana-Leibowitch, P. Fortier, J. Leibowitch, J.-P. Escande, J. Am. Acad. Dermatol. 20 (1989) 511.
[6] L. Lin, D.N. Cook, G.P. Wiesehahn, R. Alfonso, B. Behrman, G.D. Cimino, L. Corten, P.B. Damonte, R. Dikeman, K. Dupuis, Y.M. Fang, C.V. Hanson, J.E. Hearst, C.Y. Lin, H.F. Londe, K. Metchette, A.T. Nerio, J.T. Pu, A.A. Reames, M. Rheinschmidt, J. Tessman, S.T. Isaacs, S. Wollowitz, L. Corash, Transfusion 37 (1997) 423.
[7] M. Palumbio, P. Rodighiero, O. Gia, A. Guiotto, S. Marciani Magno, Photochem. Photobiol. 44 (1986) 1.
[8] A.Y. Potapenko Jr., J. Photochem. Photobiol. B 9 (1991) 1.
[9] F. Wilkinson, W. Phillip Helman, A.B. Ross, J. Phys. Chem. Ref. Data 24 (1995) 663.
[10] F. Bordin, F. Carlassare, M.T. Conconi, A. Capozzi, F. Majone, A. Guiotto, F. Baccichetti, Photochem. Photobiol. 55 (1992) 221.
[11] D.F. Eaton, Pure Appl. Chem. 60 (1988) 1107.

[12] R. Schmidt, C. Tanielian, R. Dunsbach, C. Wolff, J. Photochem. Photobiol. A 79 (1994) 11.
[13] N.J. Turro, Modern Molecular Photochemistry, University Science Books, Mill Valley, CA, 1991.
[14] A.A. Krasnovskii Jr., G.T. Khachaturova, V.V. Bulgaru, L.A. Polyakova, G.E. Krichevskii, Dok. Akad. Nauk. SSSR 285 (1985) 654.
[15] R.W. Redmond, S.E. Braslavsky, Chem. Phys. Lett. 148 (1988) 523.
[16] J. Bendig, R. Schmidt, H.-D. Brauer, Chem. Phys. Lett. 202 (1993) 535.
[17] W.M. Nau, J.C. Scaiano, J. Phys. Chem. 100 (1996) 11360.
[18] E. Oliveros, P. Suardi-Murasecco, T. Aminian-Saghafi, A.M. Braun, H.-J. Hansen, Helv. Chim. Acta 74 (1991) 79.